Helmholtz-Zentrum Geesthacht
Zentrum für Material- und Küstenforschung

Final Draft
of the original manuscript:

Krueger-Genge, A.; Braune, S.; Walter, M.; Krengel, M.; Kratz, K.; Kuepper, J.-H.; Lendlein, A.; Jung, F.:

Influence of different surface treatments of poly(Eta-butyl acrylate) networks on fibroblasts adhesion, morphology and viability

In: Clinical Hemorheology and Microcirculation (2018) IOS Press

DOI: 10.3233/CH-189130

Influence of different surface treatments of poly(*n*-butyl acrylate) networks on fibroblasts adhesion, morphology and viability

A. Krüger-Genge[1,*], S. Braune[1,*], M. Walter[1,4], M. Krengel[1,4], K. Kratz[1,2], J.H. Küpper[4], A. Lendlein[1,2,3] and F. Jung[1,2]

1. Institute of Biomaterial Science and Berlin-Brandenburg Center for Regenerative Therapies (BCRT), Helmholtz-Zentrum Geesthacht, Teltow, Germany
2. Helmholtz Virtual Institute "Multifunctional Biomaterials for Medicine", Berlin and Teltow, Germany
3. Institute of Chemistry, University of Potsdam, Potsdam, Germany
4. Institute of Biotechnology, Brandenburg University of Technology Cottbus-Senftenberg, Senftenberg, Germany

Corresponding author: Prof. Dr. F. Jung (friedrich.jung@hzg.de)

*: Both authors contributed equally.

Abstract

Background: Physical and chemical characteristics of implant materials determine the fate of long-term cardiovascular devices. However, there is still a lack of fundamental understanding of the molecular mechanisms occurring in the material-tissue interphase. In a previous study, soft covalently crosslinked poly(*n*-butyl acrylate) networks (cP*n*BA) were introduced as sterilizable, non-toxic and immuno-compatible biomaterials with mechanical properties adjustable to blood vessels. Here we study the influence of different surface treatments in particular oxygen plasma modification and fibrinogen deposition as well as a combinatorial approach on the adhesion and viability of fibroblasts.

Material and Methods: Two types of cP*n*BA networks with a Young's moduli of 0.19 ± 0.01 MPa (cP*n*BA04) and 1.02 ± 0.01 MPa (cP*n*BA73) were synthesized and post-modified using oxygen plasma treatment (OPT) or fibrinogen coating (FIB) or a combination of both (OPT+FIB). The water contact angles of the differently post-treated cP*n*BAs were studied to monitor changes in the wettability of the polymer surfaces. Because of the key role of vascular fibroblasts in regeneration processes around implant materials, here we selected L929 fibroblasts as model cell type to explore morphology, viability, metabolic activity, cell membrane integrity as well as characteristics of the focal adhesions and cell cytoskeleton on the cP*n*BA surfaces.

Results: Compared to non-treated cP*n*BAs the advancing water-contact angles were found to be reduced after all surface modifications ($p < 0.05$, each), while lowest values were observed after the combined surface treatment (OPT+FIB). The latter differed significantly from the single OPT and FIB. The number of adherent fibroblasts and their adherence behavior differed on both pristine cP*n*BA networks. The fibroblast density on cP*n*BA04 was 743 ± 434 cells · mm^{-2}, was about 6.5 times higher than on cP*n*BA73 with 115 ± 73 cells · mm^{-2}. On cP*n*BA04, about 20% of the cells were visible as very small, round and buckled cells while all other cells were in a migrating status. On cP*n*BA73, nearly 50% of fibroblasts were visible as very small, round and buckled cells. The surface functionalization either using oxygen plasma treatment or fibrin coating led to a significant increase of adherent fibroblasts, particularly the combination of both techniques, for both cP*n*BA networks. It is noteworthy to mention, that the fibrinogen coating overruled the characteristics of the pristine surfaces; here, the fibroblast densities after seeding were identical for both cP*n*BA networks. Thus, the binding rather depended on the fibrinogen coating than on the substrate characteristics anymore. While the integrity of the fibroblasts membrane was comparable for both polymers, the MTS tests showed a decreased metabolic activity of the fibroblasts on cP*n*BA.

Conclusion: The applied surface treatments of cP*n*BA successfully improved the adhesion of viable fibroblasts. Under resting conditions as well as after shearing the highest fibroblast densities were found on surfaces with combined post-treatment.

Key words: Biomaterial, poly(*n*-butyl acrylate), fibroblast, oxygen plasma, fibrinogen, cell adhesion, focal adhesion, actin cytoskeleton, viability

1. Introduction

Polymer-based biomaterials are used in medicine today e.g. for vascular prostheses, organ and vascular patches, stents, occluder devices, etc. to replace or to re-establish functions of failing tissues or organs [1]. To improve our understanding of the molecular mechanisms occurring in the material-tissue interphase, systematic studies are needed that elaborate the physical and chemical characteristics, which determine the long-term fate of these devices.

Previously, soft covalently crosslinked poly(*n*-butyl acrylate) networks (cP*n*BA) have been introduced as sterilizable, non-toxic and immuno-compatible biomaterials with adjustable mechanical properties in the range between 100 kPa and 10 MPa [2]. Nano-indentation analysis utilizing atomic force microscopy revealed that the cP*n*BA network elasticity can be defined by the degree of crosslinking and is not altered when the networks are exposed to physiological solutions, such as cell culture medium [3–5]. cP*n*BA networks were discussed to be utilized as candidate polymers for vascular implants e.g. stents or vascular prostheses, which have to provide mechanical properties adapted to the targeted tissues.

Previous studies revealed that the initial adhesion of fibroblasts and endothelial cells was delayed. Cell morphology was mostly rounded and cells were only loosely attached [5], which was discussed as a consequence of the hydrophobicity of the cP*n*BA surfaces [6]. An attachment of the endothelial cells occurred after 2 to 3 days of incubation, possibly because of a protein layer on the cP*n*BA surface, which was formed in the meantime [5].

Attachment and secretion of extracellular matrix was also shown for vascular smooth muscle cells and fibroblasts. In this study, significantly higher numbers of viable fibroblasts were found on the cP*n*BA04 surface with higher elasticity. Interestingly, numbers of adherent and viable smooth muscle cells were not influenced by this property of the polymer network [3]. Oxygen plasma or serum protein (fetal bovine serum) post-treatments of cP*n*BA networks were

described as successful techniques for reducing the advancing contact angles of such materials to values below 90° without altering the local mechanical properties [4]. Human osteosarcoma cells, for instance, adhered equivalently (same level of cell density) after both surface treatments. However, on the serum post-treated polymers, cells showed an increased level of spreading compared to cells cultured on the oxygen plasma treated samples. Despite the elasticity of the cP*n*BA, samples did not influence the adsorption of serum proteins on the pristine polymer networks, values differed after the oxygen plasma treatment. Here, more serum albumin adsorbed on the cP*n*BA samples with higher elasticity. The critical pressure needed for the detachment of the cells from these substrates was lower compared to the samples with higher elasticity [4].

From these studies, it remains unclear whether a combinatorial approach of both surface treatments leads to improved cell adhesion and reduced detachment of the cells from the substrate, independent of the elastic properties. Here, we studied the influence of a combinatorial approach of oxygen plasma treatment and fibrinogen coating on the adhesion, viability, and morphology of L929 fibroblasts on hydrophobic cP*n*BA networks with varying elastic properties.

2. Material and Methods

2.1 Materials

Synthesis, formation and physical-chemical characterization were previously described elsewhere [2,5]. In brief, poly(*n*-butyl acrylate) networks were prepared by thermally induced free radical polymerization of *n*-butyl acrylate and the low molecular weight poly(propylene glycol) dimethacrylate crosslinker (PPGDMA, M_n = 560 g · mol^{-1}; cP*n*BA04 = 0.4 wt% PPGDMA; cP*n*BA73 = 7.3 wt% PPGDMA) and subsequent purification utilizing a swelling / de-swelling approach.

As previously published by our group, the selected polymer networks possess similar integral and surface properties of non-porous films with surface roughness in the nanometer range (R_q cP*n*BA04 = 37 nm ± 10 nm, R_q cP*n*BA73 = 17 nm ± 04 nm), while their mechanical properties were different with 0.19 ± 0.01 MPa for cP*n*BA04 and 1.02 ± 0.01 MPa for cP*n*BA73 [7]. Pristine and oxygen plasma treated polymer networks were ethylene oxide sterilized (gas phase: 10 vol% ethylene oxide, 54 °C, 65 % relative humidity, 1.7 bar, gas exposure: 3 h, deaeration phase: 21 h) before any further biological experiments including FIB coating.

2.2 cPnBA surface functionalization

Following surface post-treatments were carried out to modify the cP*n*BA networks before conducting cell culture experiments: oxygen plasma treatment (OPT), fibrinogen coating (FIB), oxygen plasma and subsequent fibrinogen coating (OPT+FIB).

The oxygen plasma treatment protocol was previously reported in detail by our group [4]. In brief, samples were placed in a tubular microwave-plasma reactor system (2.45 GHz, modified Plaslan 500, JE PlasmaConsult, Wuppertal, Germany), which was evacuated (10 min, 10^{-3} mbar) and purged with oxygen (10 minutes). Oxygen plasma was ignited at 0.5 mbar pressure and polymer networks were treated at 1000 W for 120 s.

The fibrinogen coating protocol was published earlier for non-functionalized cP*n*BA networks [7]. Before and after oxygen plasma treatment, polymer networks were exposed to human fibrinogen (10 $\mu g \cdot mL^{-1}$) diluted in phosphate buffered saline solution for 24 hours at 4 °C.

2.3 Physico-chemical surface characterization

Contact angle measurements using the captive bubble method in deionized water, were carried out on a DSA 100 (Krüss GmbH, Hamburg, Germany) to explore the wettability of the sterilized pristine and post-treated samples [4]. Fibrinogen layer thickness was determined as previously

reported for untreated cP*n*BA networks [7]. For the visualization of adherent fibrinogen, a polyclonal goat anti-human fibrinogen IgG primary antibody (Abcam, Cambridge, UK) and a CY3-conjugated polyclonal donkey anti-goat secondary antibody were used (Jackson Immuno Research, Suffolk, UK). Confocal laser scanning microscopy was carried out (CLSM 510 Meta, Carl Zeiss MicroImaging, Jena, Germany) in xy (Frame scan) as well as xyz mode (Z-Stack, line modus). Five predetermined positions on each polymer sample were analyzed, with 10 measurements along each scanned line axis.

2.4 Cell cultivation

Murine fibroblasts: NCTC clone 929 [L cell, L-929, derivative of Strain L], ATCC, LGC Standards GmbH, Wesel, Germany (L929) were cultivated on tissue culture treated polystyrene (TCP, TPP, Saint Louis, US) in MEM medium (Biochrom, Merk-Millipore, Berlin, Germany) supplemented with 10 wt% horse serum (Biochrom, Merk-Millipore, Berlin, Germany). After reaching 80% confluence, L929 cells were harvested and seeded (1x 10^5 cells · mL^{-1}) on the cP*n*BA networks (13 mm diameter discs) in 24 well TCP cell culture plates (TPP, Saint Louis, US). Cells were cultivated on the functionalized (OPT, FIB, OPT+FIB) and non-functionalized cP*n*BA networks for 48 hours (each n = 8).

2.5 Cell adhesion, morphology and viability

L929 cell adhesion and morphology was monitored with an inverted microscope, equipped with a phase contrast filter (Axiovert 40C, Zeiss, Jena, Germany). After an incubation time of 48 hours, adherent cells were fixed (4 wt% paraformaldehyde, Sigma-Aldrich, Steinheim, Germany), permeabilized (0.5 wt% Triton X-100, Fluka, Sigma-Aldrich, Steinheim, Germany) and blocked (5 wt% bovine serum albumin, fraction V, Merck Millipore, Darmstadt, Germany). Cytoskeletal filamentous F-actin was stained with AlexaFluor555 conjugated phalloidin (Life Technologies GmbH, Darmstadt, Germany). Cytoskeletal vinculin - as part of focal adhesion

complexes - was labelled with a monoclonal mouse anti-human vinculin primary-antibody (clone hVIN-1, Sigma-Aldrich, Steinheim, Germany) and goat anti-mouse Cy2 conjugated secondary-antibody (Jackson ImmunoResearch, Newmarket, Suffolk, UK). Polymer networks were fixed on glass microscope slides and embedded in Mowiol® 4–88 (Polyscience Inc, Eppelheim, Germany). Microscopic evaluation of all immunocytochemically labeled samples was performed with a confocal laser scanning microscope.

Viability of the adherent cells was accessed with a life / dead cell assay [2,3]. Cells were treated with fluorescein diacetate (FDA, 25 µg · mL^{-1}, Life Technologies GmbH, Darmstadt, Germany) and propidium iodide (PI, 2 µg · mL^{-1}, Life Technologies GmbH, Darmstadt, Germany) supplemented staining medium for 5 minutes at 37 °C in a humidified atmosphere and immediately analyzed microscopically. Viable cells (FDA positive) and apoptotic or dead cells (PI positive) were visualized with CLSM.

Further evaluation of the cell viability included: tetrazolium salt reduction assays (MTS, Promega, Mannheim, Germany) to determine the activity of the cellular energy metabolism and lactate dehydrogenase release assays (LDH, Roche, Mannheim, Germany) to assess the functional integrity of the cell membrane [2].

2.6 Statistics

For all samples, mean value ± standard deviation is given. Gaussian distributions were tested for all samples using Kolmogorov and Smirnov test. For sample comparison, paired t-tests have been performed. Differences between the samples were considered significant at p values < 0.05.

3. Results

3.1 Physico-chemical characterization of cPnBA networks after surface functionalization

Dynamic contact angle measurement results and fibrinogen layer thickness of the fibrinogen coated samples are summarized in Table 1. For cP*n*BA04, advancing and receding contact angles were reduced after all surface modifications ($p < 0.05$). θ_{Adv} values ranged between 96.6 ° ± 7.6 ° and 118.7 ° ± 4.0 °, indicating an unchanged overall hydrophobic character of the network. Lowest values were observed after the combined surface treatment (OPT+FIB), which differed significantly from the OPT and FIB only approaches. Similar hydrophobic surface properties were observed for cP*n*BA73 with advancing contact angles ranging from 94.8 ° ± 3.7 ° to 104.6 ° ± 7.4 °. Fibrinogen coated cP*n*BA73 (FIB) showed the strongest decrease in the advancing contact angle and values were significantly different to the non-treated, OPT and the OPT+FIB approaches. For both cP*n*BA networks and all surface treatments, decreasing receding contact angles (θ_{Rec}) were observed, which were similar for all surface treatments (see Table 1).

Table 1. Water contact angles after different surface treatments for cP*n*BA04 and cP*n*BA73 without surface treatment (Unmodified), after fibrinogen coating (FIB) and after oxygen plasma treatment without / with fibrinogen coating (OPT / OPT+FIB) (arithmetic mean ± standard deviation).

Sample		θ_{Adv} [°]	$\theta_{Receding}$ [°]	Fibrinogen layer thickness [µm]
cP*n*BA04	Unmodified	118.7 ± 4.0	41.6 ± 2.8	-
	OPT	107.4 ± 5.3	26.3 ± 3.6	-
	FIB	106.4 ± 4.3	41.6 ± 2.8	4.3 ± 0.3
	OPT+FIB	96.6 ± 7.6	26.4 ± 4.2	5.8 ± 0.6
cP*n*BA73	Unmodified	104.6 ± 7.4	40.3 ± 6.5	-
	OPT	103.6 ± 4.2	22.4 ± 1.7	-
	FIB	94.8 ± 3.7	40.3 ± 6.5	3.8 ± 0.7
	OPT+FIB	103.3 ± 2.7	21.1 ± 0.9	2.7 ± 0.4

3.2 Immunostaining of surface bound fibrinogen

On the control samples (cP*n*BA without fibrinogen) only sparse unspecific signals occurred (Fig. 1). On cP*n*BA04, fibrinogen coating resulted in a thinner protein layer (4.3 ± 0.3 µm) compared to the OPT+FIB treated networks (5.8 ± 0.8 µm). The fibrinogen molecules were homogenously spread over the complete area of the samples. For cP*n*BA73, overall values were lower than on cP*n*BA04. Fibrinogen coating of cP*n*BA73 resulted in a thicker protein layer (3.8 ± 0.7 µm) compared to the samples coated subsequently to the oxygen plasma treatment (2.7 ± 0.4 µm).

3.3 Metabolic activity and cell membrane integrity

Table 2 shows results of the LDH test to analyze the integrity of the cell membrane as well as of the MTS test to study the metabolic activity of the fibroblasts on both polymeric networks.

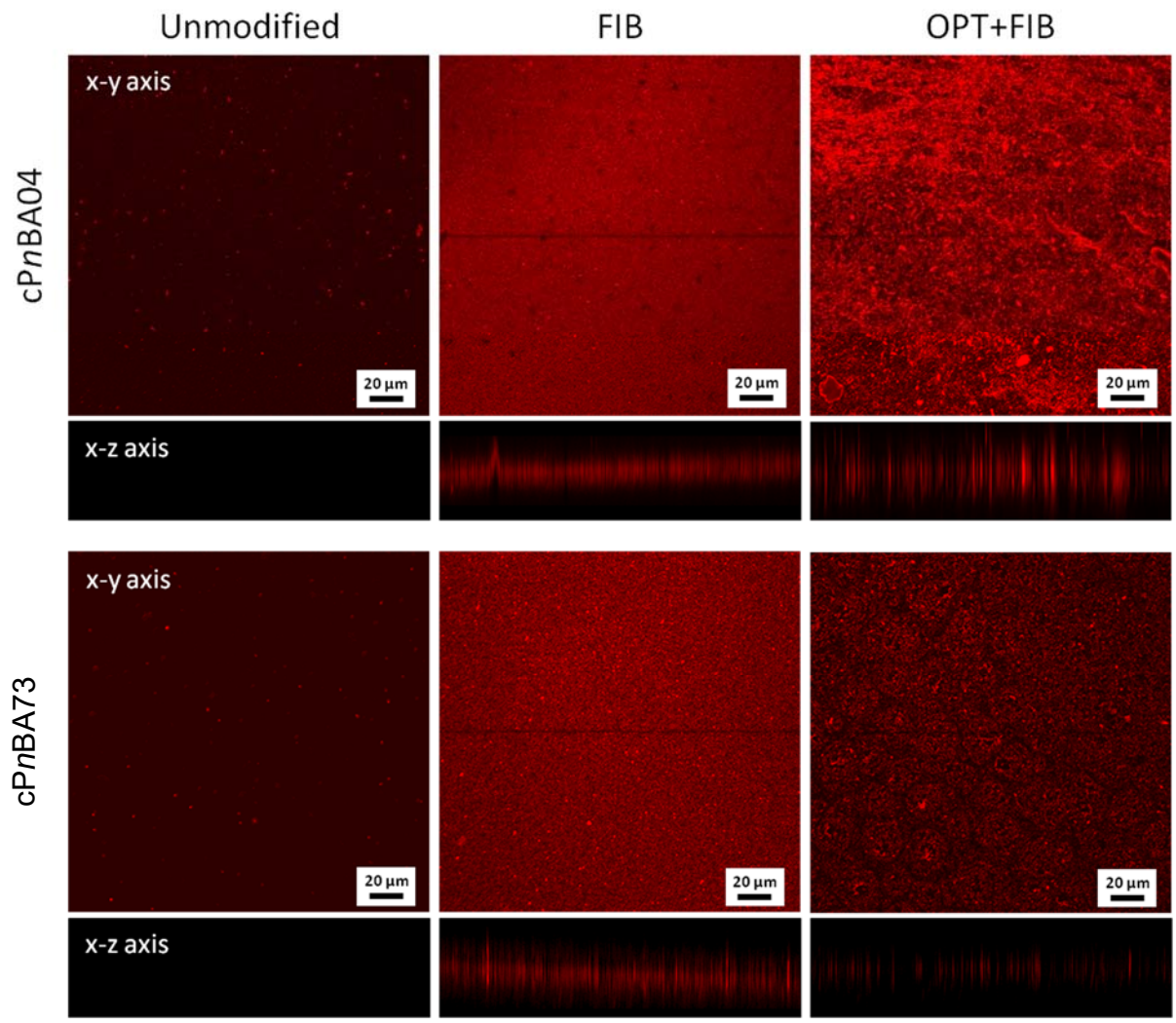

Figure 1. Representative confocal laser scanning microscopy images of surface bound fibrinogen on cP*n*BA04 and cP*n*BA73 without surface treatment (Unmodified), after fibrinogen coating (+FIB), and after oxygen plasma treatment followed by fibrinogen coating (OPT+FIB) (x-y axis images for the none treated and FIB are taken from [7], © 2011 – IOS Press and the authors).

For cP*n*BA04, the extracellular LDH levels did not differ between the unmodified polymer network and the surface functionalized samples. The LDH levels were markedly increased for cP*n*BA73 compared to the respective functionalized samples. Differences between the samples ranged between 20% - 26% and revealed a rather weak influence on the cell membrane integrity. Despite OPT+FIB treatment resulted in an increase of the metabolic activity of the adherent cells for cP*n*BA04, the overall data revealed that the functionalization did not lead to an improvement.

Table 2. Cell densities, LDH and MTS results for cP*n*BA04 and cP*n*BA73 without surface treatment (Unmodified), after fibrinogen coating (+FIB), and after oxygen plasma treatment without / with fibrinogen coating (OPT / OPT+FIB) (arithmetic mean ± standard deviation).

		Cell density [cells · mm^{-1}]	MTS [Absorption, 492 nm]	LDH [Absorption, 492 nm]
cP*n*BA04	Unmodified	743 ± 434	0.799 ± 0.053	0.226 ± 0.039
	OPT	874 ± 401	0.809 ± 0.031	0.205 ± 0.015
	FIB	808 ± 157	0.791 ± 0.053	0.213 ± 0.014
	OPT+FIB	1,454 ± 428	0.888 ± 0.076	0.205 ± 0.015
cP*n*BA73	Unmodified	115 ± 73	0.439 ± 0.088	0.287 ± 0.027
	OPT	675 ± 372	0.291 ± 0.079	0.213 ± 0.010
	FIB	755 ± 278	0.370 ± 0.074	0.228 ± 0.010
	OPT+FIB	638 ± 173	0.372 ± 0.076	0.212 ± 0.011

3.4 Viability and density of adherent fibroblasts

FDA staining revealed that the vast majority of the cells were viable and less than 0.5% PI positive cells were observed. On the softer cP*n*BA04 network, more viable cells adhered compared to cP*n*BA73 ($p<0.05$). The functionalization of cP*n*BA04 led to a slight increase of the fibroblast density, which was even more the case for the samples functionalized by OPT and FIB. The cell density was higher than for the non- or the single functionalized materials ($p<0.05$). The cell densities on cP*n*BA73 did not differ for the three functionalized surfaces; however, on all three functionalized materials the fibroblast densities were higher than on the pristine polymer network ($p<0.05$ each). Table 3 shows the number of adherent L929 fibroblasts per area on both pristine as well as the single (FIB or OPT) or the double functionalized materials (OPT+FIB) directly after cultivation and after staining and washing procedures. While 36.5% of the adherent fibroblast detached from cP*n*BA04 during the washing and staining procedure, this occurred for 17.6% of the adherent fibroblasts on cP*n*BA73 ($p=0.0041$).

Table 3. Number of adherent L929 fibroblasts per mm^2 on cP*n*BA04 and cP*n*BA73 without surface treatment (Unmodified), after fibrinogen coating (FIB), and after oxygen plasma treatment without / with fibrinogen coating (OPT / OPT+FIB) (arithmetic mean ± standard deviation).

		Cell density [cells · mm^{-1}]		
		Post cultivation	Post staining	% decrease
cP*n*BA04	Unmodified	743 ± 434	505 ± 70	-32.0
	OPT	874 ± 401	587 ± 271	-32.8
	FIB	808 ± 157	551 ± 339	-31.8
	OPT+FIB	1,454 ± 428	740 ± 99	-49.1
cP*n*BA73	Unmodified	115 ± 73	93 ± 128	-19.1
	OPT	675 ± 372	604 ± 123	-10.5
	FIB	755 ± 278	518 ± 256	-31.3
	OPT+FIB	638 ± 173	578 ± 273	-9.4

3.5 Morphology of adherent fibroblasts

Fibroblasts on pristine cP*n*BA04 showed a non-spread round or spindle-shape morphology. Only on the double functionalized surface (OPT+FIB) the cells presented with the physiological size of 30 – 50 µm in an epithelioid or polygonal morphology with two or three cytoplasmic processes, were spread and flattened and had formed typical lammelipodia / filopodia (Fig. 2). On all four surfaces nearly all fibroblasts were still migrating. Fibroblasts on the pristine cP*n*BA73 showed a different behavior; here more cells were rounded, lifted and seemed to be loosely attached. This pattern changed after functionalization. Particularly fibroblasts of the double functionalized surface showed the typical morphology and size. The cells were spread, flattened and had formed the typical lammelipodia.

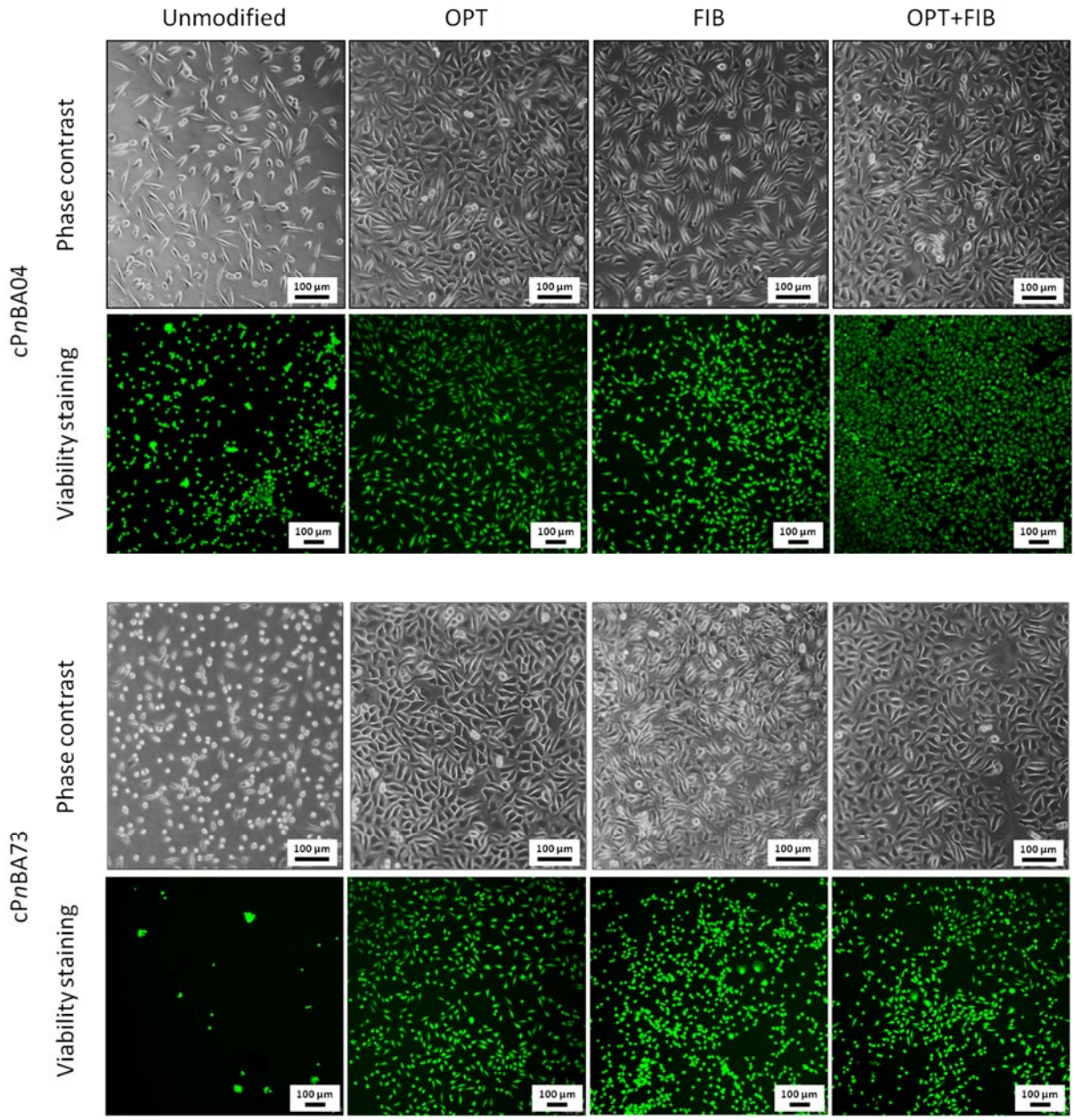

Figure 2. Representative phase contrast and viability staining (FDA / PI) images of L929 cells 48 hours after seeding on cP*n*BA04 and cP*n*BA73 networks without surface treatment (Unmodified), after fibrinogen coating (FIB) and after oxygen plasma treatment without / with fibrinogen coating (OPT / OPT+FIB).

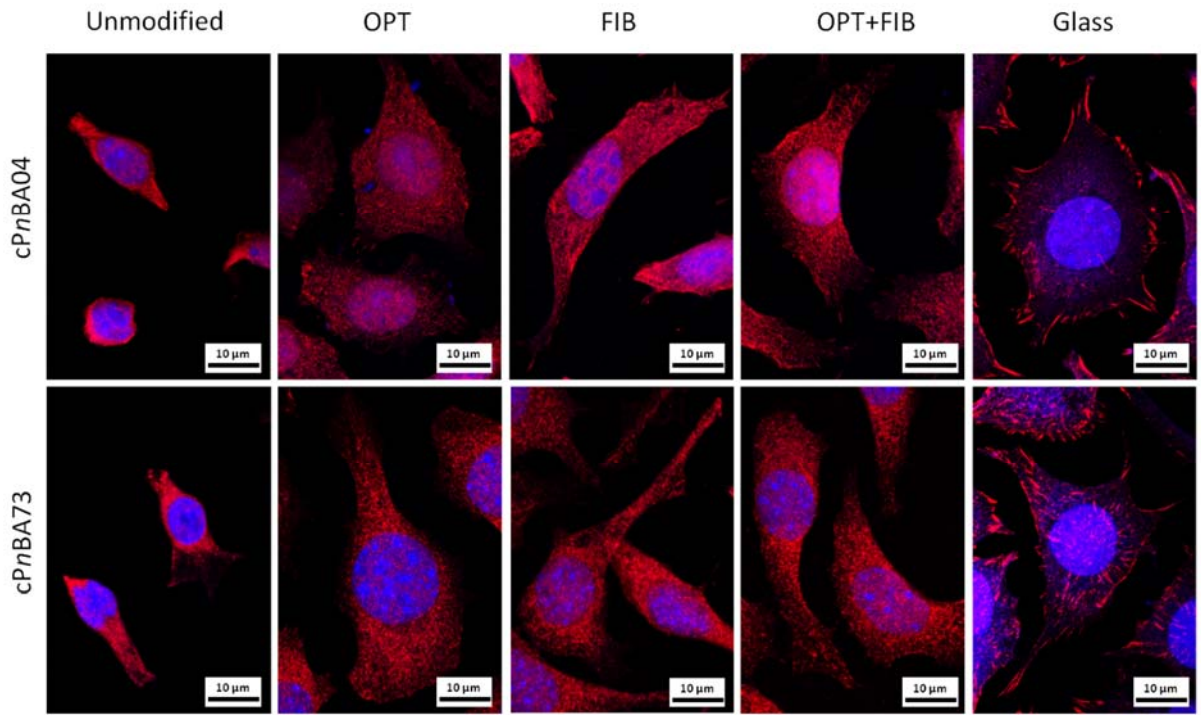

Figure 3. Representative confocal laser scanning microscopy images of focal adhesions (vinculin labeling) of L929 cells seeded on cP*n*BA04 and cP*n*BA73 without surface treatment (Unmodified), after fibrinogen coating (FIB), and after oxygen plasma treatment followed by fibrinogen coating (OPT+FIB) and coverslip glass as control.

3.6 Cell-substrate binding

Figure 3 shows fibroblasts 48 hours after seeding on the non- and functionalized cP*n*BA samples in comparison to fibroblasts seeded on glass. The distribution of vinculin for both polymeric networks is completely different from the distribution on the control (glass). While vinculin and thus focal adhesions were homogeneously spread over the basal surface of the adherent fibroblasts, on glass vinculin was more concentrated at the rim of the cells. In addition, the contact area of the cells was clearly diminished on the pristine surface; it seems that only in the cell centers focal adhesions were formed.

Figure 4 shows the actin filaments typically occurring during stress or migration. On all surfaces the cells were moving with actin microfilament bundles visible along the axis of the cells. There

seemed to be no differences between both polymers. However, fibroblasts on the functionalized surfaces covered a far smaller surface with obviously less actin bundles.

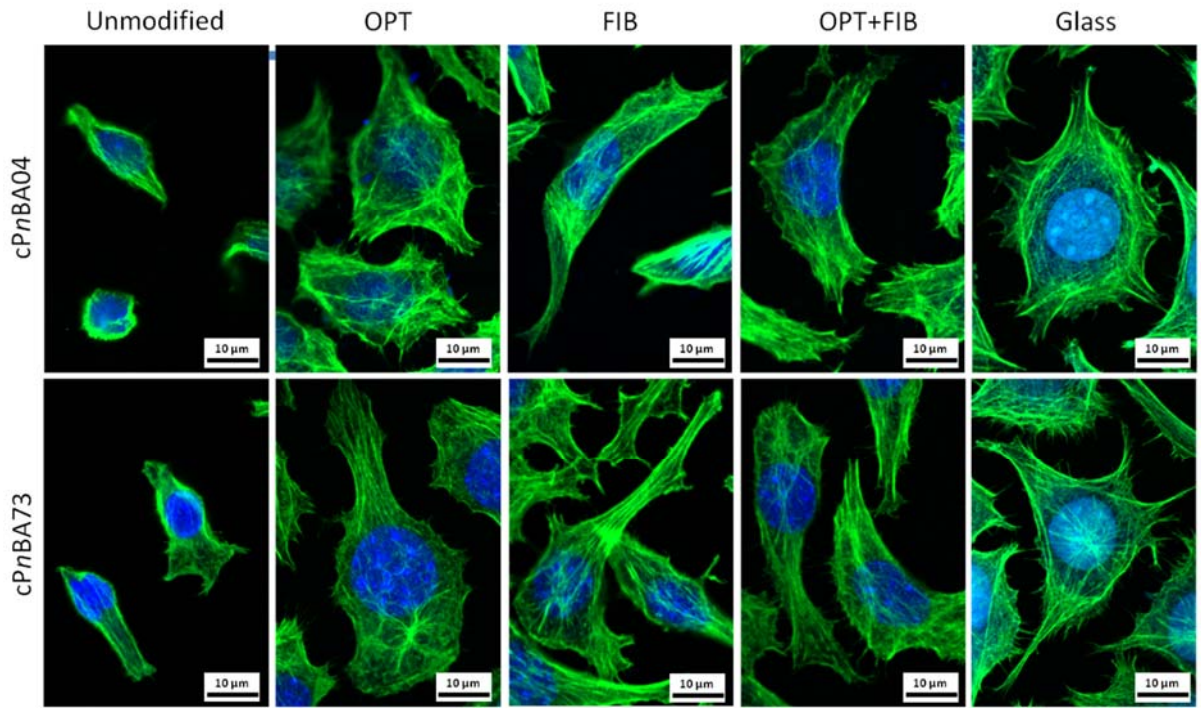

Figure 4. Representative confocal laser scanning microscopy images of F-actin fibers (phalloidin labeling) of L929 cells seeded on cP*n*BA04 and cP*n*BA73 without surface treatment (Unmodified), after fibrinogen coating (FIB), and after oxygen plasma treatment followed by fibrinogen coating (OPT+FIB) and coverslip glass as control.

4. Discussion

Fibroblasts are found in numerous tissues and are of mesenchymal origin. Products released by fibroblasts are components of the extracellular matrix (ECM) such as different types of collagen, fibronectin, and proteoglycans [8] as well as ECM-degrading enzymes. Therefore, fibroblasts play a key role in normal matrix turnover as well as in pathological matrix deposition or degradation, which can occur, for instance, during inflammation or fibrotic processes [9,10]. Because of their key role in regeneration processes around implant materials, the adhesion,

viability and morphology of fibroblasts on a newly developed polymer network – with elasticities that can be tailored to values matching those of the vascular wall – was examined.

Prior to performing experiments, all samples were sterilized and proven to have a low endotoxin content (below FDA standards of < 0.02 EU · mm^{-1} [11,12]) and were not cytotoxic (tested according to EN ISO 10993-5, [2]). The fibroblasts were analyzed 48 hours after seeding because the spreading process on planar surfaces usually is terminated after 36 to 48 hours [11]. The adherence of fibroblasts clearly differed significantly for both unmodified cP*n*BA networks (see Table 3). While the integrity of the cell membrane was comparable for both polymers (comparable LDH values), the MTS tests showed that the metabolic activity of fibroblasts seeded on cP*n*BA73 was reduced, compared to previously published data of an indirect cytotoxicity testing with the eluates of the cP*n*BA networks [5]. A decrease of the metabolic activity was found only after the direct contact of the fibroblasts with cP*n*BA73. A reason for this decrease is unclear up to now. ROS production could impair the function of the mitochondria markedly by attacking the mitochondria membrane and thereby the fission and fusion process of the mitochondria [13]. However, Mayer et al. could show that pro-inflammatory cytokines (e.g. TNF-α) were released by cells seeded on both materials (slightly more of cells on cP*n*BA04) [14,15]. Therefore, this mechanism can be excluded.

Another possible mechanism is that actin binding enhances the sensitivity to apoptotic stimuli [16], while G-actin protects against apoptosis by closing the voltage-dependent anion channel and thus retarding the release of cytochrome c [17]. Also, this mechanism can be excluded, since the formation of actin stress fibres were comparable on both materials. The significant decrease of MTS on cP*n*BA73 remains unclear.

Also, the number of adherent cells differed markedly on the unmodified networks: the fibroblast density on cP*n*BA04 was, with 743 ± 434 fibroblasts · mm^{-2}, 6.5 times higher than on cP*n*BA73 with 115 ± 73 fibroblasts · mm^{-2}. Phase contrast microscopy and confocal images showed that

the fibroblasts had difficulties to adhere or to spread, respectively, onto both polymers (see Figures 2-4). On cP*n*BA04 about 20% of the cells were visible as very small (less than 10 µm, while spread they show lengths between 30 to 50 µm), round and buckled cells while all other cells were in a migrating status. On cP*n*BA73, nearly 50% of fibroblasts were visible as very small, round and buckled cells. Moving fibroblasts detach and contract their tail processes from time to time, but later their anterior lamella spreads forward restoring their length [18]. Another example of cell rounding is during mitosis. During both conditions cells can detach. After staining and washing – which is associated with fluid shear stress – 32% of all adherent cells were detached from the pristine cP*n*BA04, while only 19.1% were detached from the pristine cP*n*BA73. The assumption that a lot of cells were only loosely tethered was confirmed by the analysis of the cell-substrate binding. The immunological staining of the fibroblasts revealed that the contact areas between basal cell surfaces with the substrate was much smaller on the pristine surfaces than on the functionalized materials; here, a very homogenous distribution of focal adhesions (stained by vinculin) over the complete basal cell was found.

The cell substrate adhesion is mediated by focal adhesions. Components of focal adhesions are various kinases, and phosphatases as well as modulators of GTP-ases and bridging proteins like vinculin [19,20]. Focal adhesions consist of a complex network of trans-plasma-membrane integrins and cytoplasmic proteins that form a plaque linking the substrate to the actin cytoskeleton. In addition, vinculin is also part of adherence junctions, which mediate the cell-cell binding. The attachment of cells to surfaces depends on appropriate binding sites, which for synthetic polymers often are missing [21]. Therefore, the adherence of cells before and after treatment of the surfaces with fibrinogen, with oxygen plasma or both functionalizations were analyzed. The study revealed that the functionalization of both cP*n*BA networks either using oxygen plasma treatment or fibrinogen coating improved the adherence of fibroblasts.

The fibrinogen coating and the oxygen plasma treatment led to an increase in density of viable adherent cells, most prominently on cP*n*BA73, compared to values of the unmodified polymer network (see Table 3). Total cell densities were comparable and independent from the elastic properties of the cP*n*BA networks, which indicates that the surface treatments overruled these characteristics in a similar manner. After fibrinogen coating, the fibroblast densities after seeding as well as the percentage of detached cells after staining and washing were identical for both cP*n*BA networks. Thus, the cell adherence depended strongly on the surface adsorbed fibrinogen molecules, while characteristics of the pristine substrate appeared to be less relevant. This was not the case after the oxygen plasma treatment. Here, 32.8% cells were detached from the cP*n*BA04, while only 10.5% of the cells were detached from the cP*n*BA04 network. These data indicate that – despite both surface treatments were similarly effective in influencing the adhesion of the fibroblast – after oxygen plasma treatment, cells seemed to be capable of sensing the substrate elasticity stronger than after fibrinogen coating.

Oxygen plasma treatment is a widespread used method to render hydrophobic surface hydrophilic [21]. The reactions of radicals formed in an oxygen plasma with poly(*n*-butyl acrylate) surfaces is reported to predominantly generate hydroxyl, aldehyde, carbonyl or carboxyl groups via oxidation of the aliphatic *n*-butyl side chains [22] and these newly generated hydrophilic groups result in an decrease of the contact angle [4]. Among the newly generated functional groups aldehydes and ketones are capable to further react with amines forming an imine or Schiff base. Thus it can be speculated that some covalent binding of proteins to the modified cP*n*BA surfaces might occur besides the physical coating. It was interesting to see, that though the contact angles were only slightly lower and still in the high hydrophobicity range (for both materials over 100 °) the density of fibroblasts increased markedly (cP*n*BA04: from 743 ± 434 to 874 ± 401; cP*n*BA73: from 115 ± 73 to 675 ± 372

L929 fibroblasts · mm^{-2}). These increases cannot be attributed to the minor changes of the wettability but seemed to rather reflect the elastic properties of the cP*n*BA networks.

The surface treatment using oxygen plasma with fibrinogen coating was the most effective way to increase the density of fibroblasts on both materials. Highest densities of viable cells were observed for cP*n*BA04, which might be correlated to the thicker protein layer compared to all other fibrinogen coated polymer samples. Morphology, distribution of the focal adhesion points and formation of F-actin fiber formation revealed strongly migrating cells, which was independent from the elastic properties of the cP*n*BA networks and in good agreement with the respective single surface treatments.

Interestingly, differences between cP*n*BA04 and cP*n*BA73 in cell detachment were similar to the results after single oxygen plasma treatment. This indicates that the fibrinogen coating influenced the adhesion of the fibroblasts but not the binding strength of the cells (as could be seen after the washing process). The latter seemed to be more dependent on the oxygen plasma treatment. However, highest numbers of adherent and shear resistant viable fibroblasts were observed after the combinatorial surface treatment approach for cP*n*BA04. In contrast, all surface treatments induced a stronger increase in cell fibroblast densities for cP*n*BA73.

5. Conclusion

The applied surface treatments of cP*n*BA increased successfully the density of adherent fibroblasts. Under resting conditions as well as after washing-induced shearing the highest densities of viable fibroblast were found after oxygen plasma treatment and subsequent fibrinogen coating functionalization.

Acknowledgements

This work was financially supported by the Federal Ministry of Education and Research, Germany (grant no. 13GW0098), by the Ministry for Science, Research and Cultural Affairs of Brandenburg through the grant of the joint project "Konsequenzen der altersassoziierten Zell- und Organfunktionen" of the Gesundheitscampus Brandenburg, and the Helmholtz-Association (programme-oriented funding, SO-036 and grant no. VH-VI-423)

This paper is dedicated to the 70th birthday of Prof. Friedrich Alfons Jung.

References

[1] Jung F, Wischke C, Lendlein A. Degradable, Multifunctional Cardiovascular Implants: Challenges and Hurdles. MRS Bull. 2010;35(8):607–13.

[2] Cui J, Kratz K, Hiebl B, Jung F, Lendlein A. Soft poly(n-butyl acrylate) networks with tailored mechanical properties designed as substrates for in vitro models. Polym Adv Technol. 2011;22(1):126–32.

[3] Krüger A, Braune S, Kratz K, Lendlein A, Jung F. The influence of poly(n-butyl acrylate) networks on viability and function of smooth muscle cells and vascular fibroblasts. Clin Hemorheol Microcirc. 2012;52(2–4):283–94.

[4] Yoshikawa HY, Cui J, Kratz K, Matsuzaki T, Nakabayashi S, Marx A, et al. Quantitative evaluation of adhesion of osteosarcoma cells to hydrophobic polymer substrate with tunable elasticity. J Phys Chem B. 2012;116(28):8024–30.

[5] Hiebl B, Cui J, Kratz K, Frank O, Schossig M, Richau K, et al. Viability, Morphology and Function of Primary Endothelial Cells on Poly(n-Butyl Acrylate) Networks Having Elastic Moduli Comparable to Arteries. J Biomater Sci Polym Ed. 2011;23(7):901–15.

[6] Grinnell F, Feld MK. Fibronectin Adsorption on Hydrophilic and Hydrophobic Surfaces Detected By Antibody-Binding and Analyzed During Cell-Adhesion in Serum-Containing Medium. J Biol Chem. 1982;257(9):4888–93.

[7] Braune S, Hönow A, Mrowietz C, Cui J, Kratz K, Hellwig J, et al. Hemocompatibility of soft hydrophobic poly(n-butyl acrylate) networks with elastic moduli adapted to the elasticity of human arteries. Clin Hemorheol Microcirc. 2011;49(1):375–90.

[8] Spinale FG. Myocardial matrix remodeling and the matrix metalloproteinases: Influence on cardiac form and function. Physiol Rev. 2007;87(4):1285–342.

[9] Anderson JM, Rodriguez A, Chang DT. Foreign body reaction to biomaterials. Semin Immunol. 2008;20(2):86–100.

[10] Klopfleisch R, Jung F. The pathology of the foreign body reaction against biomaterials. J Biomed Mater Res Part A. 2017;105(3):927–40.

[11] Roch T, Cui J, Kratz K, Lendlein A, Jung F. Immuno-compatibility of soft hydrophobic poly (n-butyl acrylate) networks with elastic moduli for regeneration of functional tissues. Clin Hemorheol Microcirc. 2012;50(1–2):131–42.

[12] Gorbet MB, Sefton M V. Endotoxin: The uninvited guest. Biomaterials. 2005;26(34):6811–7.

[13] Jendrach M, Pohl S, Vöth M, Kowald A, Hammerstein P, Bereiter-Hahn J. Morpho-dynamic changes of mitochondria during ageing of human endothelial cells. Mech Ageing Dev. 2005;126(6–7):813–21.

[14] Mayer A, Roch T, Kratz K, Lendlein A, Jung F. Pro-angiogenic CD14(++) CD16(+) CD163(+) monocytes accelerate the *in vitro* endothelialization of soft hydrophobic poly (n-

butyl acrylate) networks. Acta Biomater. 2012;8(12):4253–9.

[15] Mayer A, Kratz K, Hiebl B, Lendlein A, Jung F. Interaction of angiogenically stimulated intermediate CD163+ monocytes/macrophages with soft hydrophobic poly(n-butyl acrylate) networks with elastic moduli matched to that of human arteries. Artif Organs. 2012;36(3):E28-38.

[16] Tang HL, Le A-HP, Lung HL. The increase in mitochondrial association with actin precedes Bax translocation in apoptosis. Biochem J. 2006;396(1):1–5.

[17] Kusano H, Shimizu S, Koya RC, Fujita H, Kamada S, Kuzumaki N, et al. Human gelsolin prevents apoptosis by inhibiting apoptotic mitochondrial changes via closing VDAC. Oncogene. 2000;19(42):4807–14.

[18] Dunn GA, Zicha D. Dynamics of fibroblast spreading. J Cell Sci. 1995;108:1239–49.

[19] Zamir E, Geiger B. Molecular complexity and dynamics of cell-matrix adhesions. J Cell Sci. 2001;114:3583–90.

[20] Giancotti FG, Ruoslahti E. Integrin signaling. Science. 1999;285(5430):1028–32.

[21] Yamamoto A, Mishima S, Maruyama N, Sumita M. Quantitative evaluation of cell attachment to glass, polystyrene, and fibronectin- or collagen-coated polystyrene by measurement of cell adhesive shear force and cell detachment energy. J Biomed Mater Res. 2000;50(2):114–24.

[22] Kawabe M, Tasaka S, Inagaki N. Effects of surface modification by oxygen plasma on peel adhesion of pressure-sensitive adhesive tapes. J Appl Polym Sci. 2000;78(7):1392–401.